

Global estimation of post-fire soil erosion

Received: 11 December 2024

Accepted: 5 November 2025

Published online: 5 January 2026

 Check for updatesD. C. S. Vieira¹✉, P. Borrelli², S. Scarpa³, L. Liakos⁴, C. Ballabio¹ & P. Panagos¹

Wildfires affect land surface and post-fire geomorphological activity worldwide, increasing surface runoff and soil erosion. However, a global quantitative assessment considering the cumulative effect of several wildfires is still missing. Here we present a global assessment of post-fire soil erosion, considering cumulative wildfire-driven geomorphological changes over the last two decades. We estimate global trends of post-fire soil erosion using a global database on wildfire occurrence and fire severity, and the Revised Universal Soil Loss Equation (RUSLE) model together with the recovery of those burned landscapes by remote sensed data. Our results show that when considering multiple wildfire events, global post-fire soil erosion accounts for 8.1 ± 0.72 Pg annually, representing 19% of the global soil erosion budget and an additional 5.1 ± 0.56 Pg soil erosion annually in comparison to pre-fire conditions. Moreover, soil erosion attributed to the first post-fire year represents 31% of the total soil erosion, whereas the remaining share can be attributed to previous wildfire occurrences. Globally, Africa is the continent that is impacted the most in terms of post-fire soil erosion, given its substantially larger burned area. Our results illustrate the magnitude of post-fire soil erosion globally and therefore support post-fire management actions towards the mitigation and restoration of affected areas and policies towards land-degradation neutrality.

According to the Global Wildfire Information System¹, on average, four million km² of land burn every year (2002–2023), an area almost equal to the European Union. Wildfires are an integral part of many ecosystems around the globe, playing key roles in ecosystem dynamics and retention of species that have evolved in response to fire². However, this global phenomenon is often responsible for environmental, social and economic losses, which combined with land abandonment, droughts, absence of appropriate land management and urban development are expected to aggravate land degradation^{3,4}. In addition, wildfires will become a persistent threat because fire risk is expected to increase in a context of a warmer and drier climate⁵.

Led by elevated temperatures in topsoil, fire-induced changes in soil physical and chemical properties reduce water infiltration and ground-cover protection and alter soil aggregate stability^{6,7}. When combined, these factors result in significant increases in soil erodibility, varying between geographical regions and burn severity^{8,9}. High-severity burns increase on-site soil erosion but also lead to offsite

impacts downstream of the burned area in the form of destructive floods and debris flows^{6,10} and transport of ash and sediment into downstream water bodies^{11,12}. Moreover, the importance of post-fire soil erosion events is likely to increase in response to ongoing and anticipated increases in fire activity and rainfall intensity¹⁰.

Wildfires have been regarded as a hydrological and geomorphological agent⁷; until now post-fire soil erosion mostly has been assessed from plot to catchment scale by means of field measurements and from slope to regional scales using modelling approaches¹³. Global-scale studies, however, have the potential to compare impacts of fires in different biomes^{10,14,15} and to put into perspective land-management actions¹⁶. Current model-based soil erosion assessments at global scales^{17,18} already gave steps forward, providing this knowledge for informed land-management decisions, however, these have not yet considered the effects of wildfires. Whereas initial large-scale post-fire soil erosion estimates⁸ provide an idea of the impact of wildfires in European soils, this approach remains limited to a single disturbance

¹European Commission, Joint Research Centre (JRC), Ispra, Italy. ²Environmental Geosciences, University of Basel, Basel, Switzerland. ³EUROPEAN DYNAMICS Luxembourg S.A, Luxembourg, Luxembourg. ⁴UNISYSTEMS, Bertrange, Luxembourg. ✉e-mail: diana.simoese-vieira@ec.europa.eu

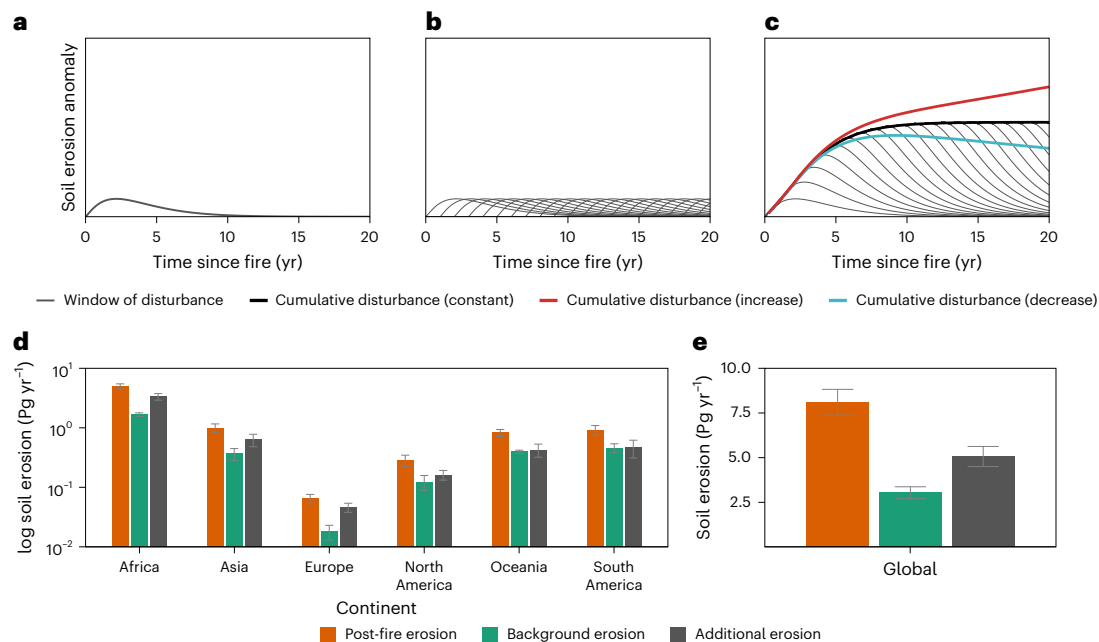


Fig. 1 | Concept of cumulative post-fire impacts and mean annual estimates of background and post-fire soil erosion for the period 2006–2019. **a**, The window of disturbance model for a single fire event⁷, where post-fire soil erosion increases after the fire and decreases with recovery. **b**, The window of disturbance for multiple wildfires with similar impacts if considered individually. **c**, The cumulative impact, achieving a plateau if impacts are similar (black line) and two alternative patterns indicating potential degradation (red line) whereas this plateau is achieved later or a positive recovery (blue line) indicating a decrease in impacts with time. **d**, Mean annual post-fire soil erosion estimates by continent (logarithmic scale). **e**, Mean annual post-fire soil erosion estimates globally (Table 1). Error bars represent standard deviation ($n = 13$). Post-fire erosion (orange bars) refers to the estimated soil loss following fire, accounting

for fire-induced changes and based on ground-cover observations. These values serve as important references for emergency response and mitigation measures in fire-affected areas. Background erosion (green bars) represents the estimated soil erosion under undisturbed vegetation conditions before fire. These estimates consider all areas affected by fires but use pre-fire conditions for parameterization. This provides reference values for soil erosion under natural, undisturbed conditions. The difference between post-fire and background erosion estimates (shown as grey bars) represents the increase in erosion attributable to fire events because of ground-cover removal and fire-induced changes in soil properties. This approach enables assessment of post-fire erosion trends independent of local intrinsic factors such as topography, soil properties and climate.

(one fire year) and a short recovery period (five years), showing that a global assessment accounting for cumulative fire impacts and a long-term perspective is still missing^{8,10}.

Hence the aim of this study is to provide the estimation of post-fire soil erosion at a global scale and to analyse geomorphological changes driven by fire over the past two decades under a land-management perspective. To accomplish this, we estimated the global post-fire soil erosion by adapting the Revised Universal Soil Loss Equation (RUSLE) model to account for cover changes induced by global wildfires. We used the largest global burn severity database available (MOSEV¹⁹) for an 18-year period and compared it against unburned conditions. This allowed to estimate the cumulative impact of several wildfire occurrences in the global soil erosion budget and identify the main trends for post-fire soil erosion at continental scale. Additionally, this allowed us to analyse the recovery of fire-affected ecosystems under systematic pressure, but also project trends into the future in combination with the anticipated changes in rainfall.

Results

Burned area, severity and erosion

Over the study area and period, annual burned areas averaged 2.9 million km². Throughout 18 years, the trend in burned areas has been declining significantly globally (Mann–Kendall trend test $p < 0.0005$), with the exception of an increase in North America (Extended Data Fig. 1). Africa is the most-affected continent, with 66% of the annual burned area identified mostly among low (67%) and moderate (33%) severities. High-severity burns are more pronounced in North America (10%), Asia (5%) and Europe (4%) but are rare in other continents (Extended Data Fig. 1).

Burned area and severity were used as inputs for soil erosion estimations with RUSLE. However, to account for the long-term contribution of fires to the global erosion budget, our estimations consider the cumulative effect of various wildfires. Therefore, we have estimated the post-fire soil erosion from each individual fire, in every fire-affected pixel throughout the 18-year timeframe, summing up the erosion amounts at annual scale (Fig. 1a–c).

To evaluate the mean and trends of post-fire soil erosion, we identified six years as the minimum period needed to capture the cumulative effects. This was estimated through the time to reach a plateau for background erosion (unburned conditions) and within the range of observed temporal effects provided by literature^{6–8}. Using this metric, the fire-affected areas targeted in this study are estimated to result in 8.1 ± 0.72 Pg of soil losses annually over 2006–2019 (Table 1 and Fig. 1d). This value represents an additional 5.1 ± 0.56 Pg of soil losses annually when compared to background soil erosion (Fig. 2). The global erosion budget revealed that only 31% (2.50 Pg yr⁻¹) of the annual soil erosion can be attributed to the most recent fire year, whereas the remaining results from previous fire events (Table 1).

Global post-fire erosion is mostly driven by African burned areas (Table 1 and Figs. 1 and 2), which corresponds to 62% of the soil losses, followed by Asia (12%), South America (11%) and Oceania (10%), with minor contributions from North America (4%) and Europe (1%) (Fig. 3), resulting in a global soil erosion rate of 9.53 Mg ha⁻¹ yr⁻¹ for the first post-fire year (Supplementary Section 1). Post-fire soil erosion estimates are mostly originated from tropical, savannah (60%) climatic zones, which are the largest contributor to erosion across most continents (Table 1). In Europe, the dominant climate types contributing to

Table 1 | Mean annual soil erosion in Pg yr⁻¹ for post-fire, background and additional erosion per continent and at global scale

	Post-fire erosion		Background erosion		Additional erosion		Statistics for post-fire soil erosion						
	Mean soil erosion	s.d.	Mean soil erosion	s.d.	Mean soil erosion	s.d.	Global	First fire year	Top contributing climatic zones				
	(Pg yr ⁻¹)		(Pg yr ⁻¹)		(Pg yr ⁻¹)		(%)	(%)	(%)/Climate classification				
Africa	5.01	0.47	1.67	0.11	3.34	0.42	62	34	66/Aw	13/Cwa	9/Cwb	6/BSh	3/Am
Asia	1.00	0.17	0.37	0.08	0.63	0.15	12	25	40/Aw	23/Cwa	7/Dwc	6/Am	3/Af
Europe	0.06	0.01	0.02	0.00	0.05	0.01	1	18	23/Dfb	21/Csa	16/Csb	14/Dfa	13/BSk
North America	0.29	0.06	0.12	0.04	0.16	0.03	4	18	17/Aw	14/BSk	10/Dfc	9/Csb	9/Cfa
Oceania	0.82	0.11	0.40	0.02	0.43	0.11	10	29	48/Aw	35/BSh	11/BWh	2/Cfa	2/Cfb
South America	0.92	0.17	0.46	0.08	0.46	0.15	11	26	74/Aw	11/Am	4/Cfa	2/Cwb	2/BSk
Global	8.1	0.72	3.0	0.33	5.1	0.56	100	31	60/Aw	12/Cwa	8/BSh	7/Cwb	4/Am

s.d. stands for standard deviation ($n=13$). Note the breakdown of post-fire soil erosion by share of global, share of first post-fire year and by top contributing climatic zones. Climatic zones⁴⁹: Af–tropical, rainforest; Am–tropical, monsoon; Aw–tropical, savannah; BSh–arid, steppe, hot; BSk–arid, steppe, cold; BWh–arid, desert, hot; Cfa–temperate, no dry season, hot summer; Cfb–temperate, no dry season, warm summer; Csa–temperate, dry summer, hot summer; Csb–temperate, no dry season, warm summer; Cwa–temperate, dry winter, hot summer; Cwb–temperate, dry winter, warm summer; Dfa–cold, no dry season, hot summer; Dfb–cold, no dry season, warm summer; Dfc–cold, no dry season, cold summer; Dwc–cold, dry winter, cold summer.

soil erosion are cold, no dry season, warm summer; and temperate, dry summer, hot summer, with similar (21–23%) share (Table 1).

Post-fire recovery and long-term soil erosion trends

Within our study it was possible to assess recovery of the affected land through the RCOVER⁸, which represents the progress of vegetation recovery when compared to pre-fire conditions. As expected, the overall recovery dynamics at continental scale reveal complex pattern whereas factors such as burn severity, ecosystem resilience and post-fire climate play major roles¹⁰.

Results show that following a single fire, continents such as Oceania and South and North America present the highest recovering performance, whereas Europe and Africa reveal modest recovery rates (Fig. 3). Additional disturbances beyond wildfires might interfere with recovery, thus explaining why the maximum recovered areas after a single fire event was as much as 83% for Oceania, 75–76% for North and South America, 67% for Asia, 56% for Europe and 46% for Africa. These results should also include the effect of precise management actions, such as logging or post-fire mitigation measures²⁰ through visible changes in vegetation indices.

When investigating recovery considering cumulative impact over several fire years (Extended Data Fig. 2), the complexity between affected land cover, climate and biome emerge. At a global level, recovered areas represent 39% of the 2019 baseline, whereas areas under high level of pressure (RCOVER [0.0–0.3]) stand in the 13% (Extended Data Fig. 2d). However, these values tend to be more favourable in forest-dominated landscapes (Recovered = 44%, [0–0.3] = 5%) or the contrary as is the case in mixed land cover (Recovered = 36%) or grassland areas ([0–0.3] = 17%). The most-affected climate (Aw, 41%) or biome (TSGSS, 54%) seems to drive global RCOVER distribution (Recovered = 33–35%, [0–0.3] = 11%).

These results suggest that burned areas not only are vulnerable immediately after the fire, but also a substantial portion of them never managed to recover to pre-fire conditions, as shown by the 39% recovered areas when considering long and recent fire impacts (Extended Data Fig. 2d) or of 48% recovery for areas burned 6 to 18 years (Fig. 3). As a result, the estimated additional soil erosion shows an increasing trend (Fig. 4), contradicting with the overall burned-area reduction trend. At a continental level, the increasing trend in annual post-fire soil erosion is only statistically significant for North America (Mann–Kendall trend test $p < 0.05$), whereas the increasing trend for Africa, Europe and Oceania, and the declining trend for Asia and South America, are statistically non-significant.

Unexpectedly, it was not possible to determine a standard recovery time within the areas affected by fire under this methodology, nor under the time range (2–7 years) provided by the scientific community^{6,7,10}. This analysis was explored under vegetation indices but also in terms of soil erosion estimations; however, FCOVER observations from before and after the fire revealed differences even in the longest time series available (2001 to 2019) after a single fire (38–69% recovery), illustrating the variability of time required to achieve recovery for fire-affected ecosystems, which can also be a result from additional disturbances besides the fire, such as land management⁸, pest outbreaks²¹ or droughts^{10,22}, which have not been considered in this study.

Future projections

Using 2019 as baseline year, we have assessed the impact of the expected changes in rainfall erosivity²³, combining changes in rainfall amounts and intensities (Extended Data Figs. 3 and 4). The computation of all Representative Concentration Pathway (RCP) scenarios results in an increase in soil erosion globally from 11% (RCP2.6) to 23% (RCP8.5) for 2050 and from 23% (RCP2.6) to 28% (RCP8.5) for 2070. The greatest contribution comes from Africa where the burned areas have a larger surface, resulting between 54% (RCP8.5) and 60% (RCP2.6) of the total post-fire soil erosion globally in 2050 and between 54% and 55% for 2070. The increase in rainfall erosivity in the burned areas in Asia, however, results in the highest relative increases between 45% and 52% for 2050 and 49% and 67% for 2070 in relation to the baseline.

Discussion

The results from this study indicate that soil erosion following wildfires worldwide represent 19% of the latest global soil erosion estimation and 35% of the soil erosion generated in agricultural land¹⁷. This global estimation can illustrate the dimension of the problem and trigger the development of solutions to prevent further impacts^{10,24}.

Despite being based in field data⁸, the comparison and validation of post-fire soil erosion estimations with field measurements is still challenging. Most of the post-fire soil erosion-monitoring field studies are focused on short-term assessments^{8,20}, whereas over long(er) terms, they have only been done as non-continuous assessments^{25,26}, often targeting processes that are scale dependent¹⁰. Fewer studies consider the impacts of various fires in soil erosion rates²⁷ nor consider the history of prior disturbances in the experimental design²⁸. The predicted global soil erosion rates for the first post-fire year (9.53 Mg ha⁻¹ yr⁻¹) are one to two orders of magnitude above the tolerable soil losses

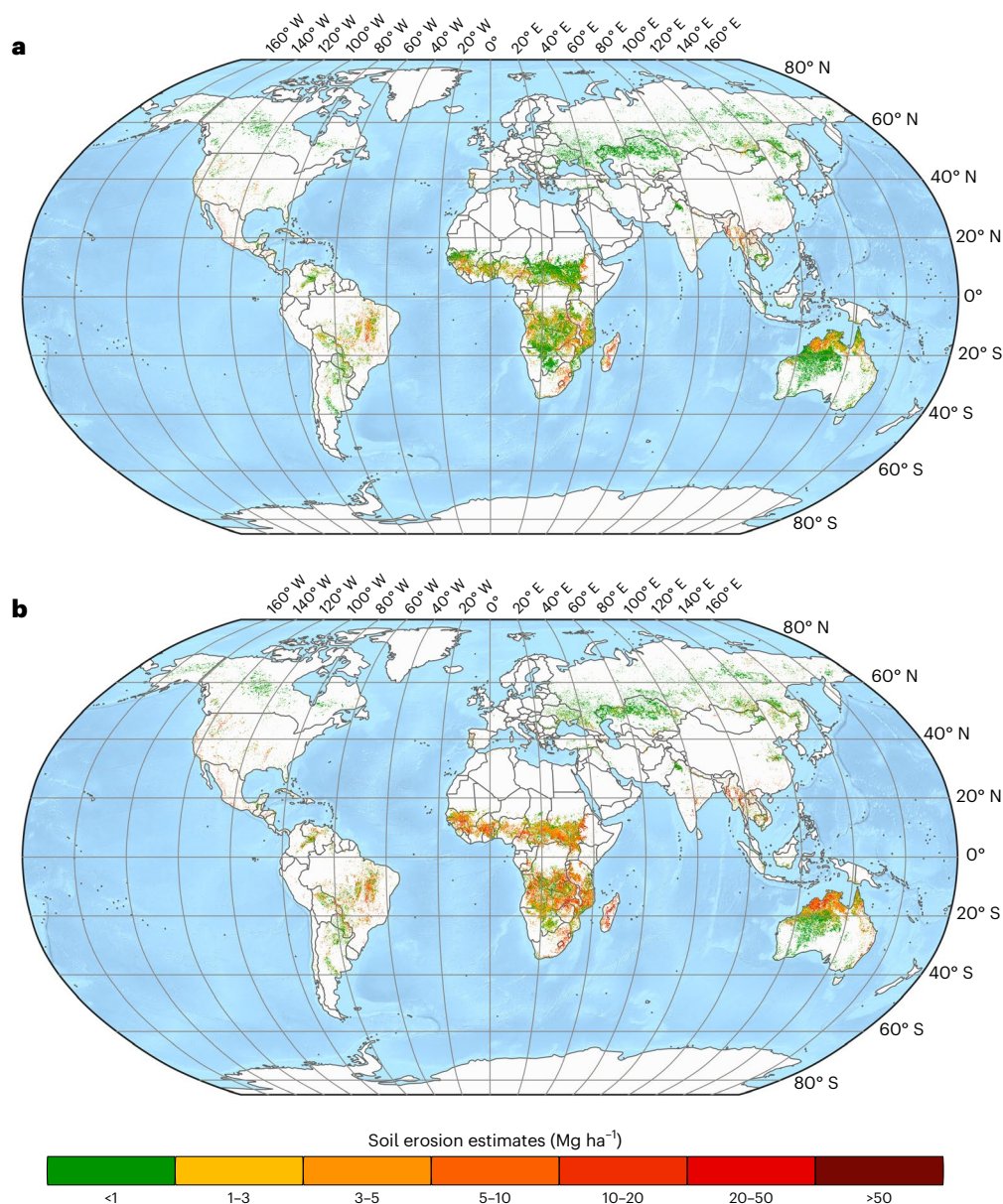


Fig. 2 | Global pre-fire and post-fire soil erosion for the year 2019. a, Global pre-fire soil erosion estimates. **b,** Global post-fire soil erosion estimates. The model provides erosion estimates for burned areas and cumulative impacts since 2001, covering land surfaces across 177 countries and approximately 12% of Earth's

terrestrial area. Soil erosion rates are categorized into seven classes based on the European Soil Bureau classification and the Global Soil Erosion Modelling Framework (GloSEM)¹⁸. Basemaps from Natural Earth (naturalearthdata.com) (projected coordinate system: sphere Robinson). Data from ref. 50.

(0.3–1.4 Mg ha⁻¹ yr⁻¹)²⁹, which is a frequently used metric in the assessment of soil health in European soils³⁰.

To assess the robustness of our estimations, we have compared those against post-fire soil erosion field observations from plot to catchment scale^{20,30}. Measured data shows a notable variability from no response to several orders of magnitude in soil erosion rates measured under different burn severities, monitoring periods and within individual countries (Fig. 5). Our estimations at country level for first post-fire year are within the range of most field observations, with some possible overestimations (Australia, Portugal and North Korea). It should be highlighted this is not an exhaustive dataset (Supplementary Section 2) and that the global post-fire soil erosion-measurements dataset is still missing¹³.

The use of RUSLE in the assessment of post-fire soil erosion globally might represent only a portion of the post-fire impacts in geomorphic processes occurring after a fire¹³. Whereas RUSLE can grasp the most

frequent hillslope processes occurring after a fire^{7,10} (sheet, inter-rill and rill erosion), estimating the potential of sediment transport to channels, it lacks connectivity and temporal scale to address processes at larger spatial scales such as mass movements¹⁰ (for example, debris flows, landslides) or sediment transport and deposition. Additionally, model adaptation to burn conditions still require further refinement on the impact of fire-induced changes to soil erodibility¹³ and how these factors change with time. Simultaneously, this approach allows the identification of areas with higher risk for erosion and therefore allows a prioritization of hotspots for the application of land-management actions^{13,31}, while its connection to other models at smaller timescales and with higher spatial resolution would allow prediction of high-risk events with consequences offsite from the burned area^{11,32,33}.

Regarding the use of MOSEV as a model input, this methodology can induce some underestimation by not identifying burned areas with sizes inferior to 25 ha (Supplementary Section 3). Despite

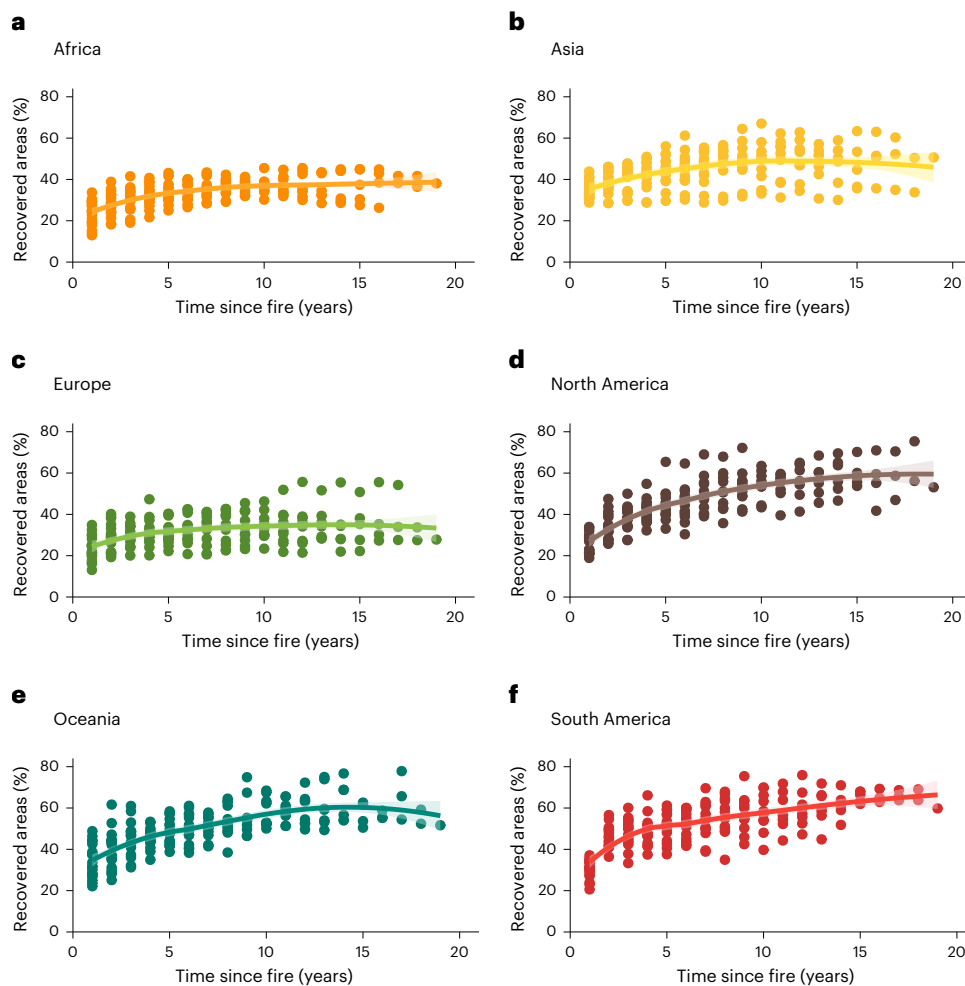


Fig. 3 | Mean recovered areas by time since fire per continent. a–f, Dots concern average share of recovered areas (%) for given time since fire (years) between 2001 and 2019 and per continent: Africa (a), Asia (b), Europe (c), North America (d), Oceania (e) and South America (f). Line expresses tendency of data by locally weighted smoothing; shaded area represents standard error with 0.95

confidence interval (ggplot2, RStudio). Recovered areas are defined as areas that achieve pre-fire vegetation cover conditions. RCOVER is determined for each continent following a single fire event and throughout the study period. Recurrent fires in the same pixel were removed from long-term assessment and reclassified as another event.

acknowledging that large fires drive most of the impacts³⁴, the size of the fire is relevant for global fire regimes and a key attribute in the definition of pyromes³⁵. We highlight the importance of having available high-resolution data on fire occurrence, burned area and burn severity at global scale for a more accurate impact assessment, similarly to what is currently being done at EU scale¹. The limited vegetation recovery observed in this study, especially for Europe and Africa, is in line with previous research²² on European forests, evidencing increasing trends of forest disturbances, such as drought or abiotic factors. This is also highlighted at global scale³⁶, indicating a reduction of forest resilience under managed and intact forests. Under this work³⁶, it was hypothesized that current (2000–2020) observed changes in forests globally could already be a result of climate-induced changes. Nonetheless, within this work it was not possible to find a comprehensive study integrating multiple local forest disturbances and to assess how such pressures interact altogether globally²¹ to fully justify the limited recovery found. In contrast, our observations for limited recovery are not aligned with others³⁷, using Enhanced Vegetation Index (EVI) and Kernel Normalized Differential Vegetation Index (kNDVI) indices to assess vegetation recovery, which observed a regain of vegetation productivity to pre-fire levels in 87% of the fire-affected areas within 2 years. Such inconsistencies might be related to differences in the definition of recovery ('Adaptation for post-fire conditions' section in Methods), differences in the indicators since FCOVER targets

ground cover, but also to the coarser scale used (10 km) in comparison with this study (500 m).

The concept of window of disturbance model³⁸ already has been extensively investigated by the post-fire community^{6,7,39} and still drives research questions on the post-fire hydrological and erosive response⁴⁰ and post-fire recovery for soil properties⁴¹. However, and similar to what was found in this study, no clear standard recovery time has been found yet. In fact, the results of this study are in line with the recently suggested geomorphic resilience framework¹⁰, whereas after wildfires, the ecosystem response can persist, change and recover or lead to an alternate state. On the basis of our results, either 18 years of observations do not allow us to fully capture the change and recovery of fire-affected areas or the share of areas under alternate state might be greater than anticipated (> 50%). In addition, the variability in climate, vegetation type, burn severity and history of past disturbances are known to affect post-fire recovery and thus explain the observed recovery variability.

The results of this study also show a non-significant statistical trend of increasing post-fire soil erosion globally despite the decreasing burned area observed from 2001 to 2019. This may be driven by a global (non-significant) increase in burn severity⁴² but also by the limited recovery of some areas as a potential consequence of land degradation⁴. Moreover, post-fire soil erosion is estimated to aggravate in the future, as 2050–2070 projections indicate an increase of

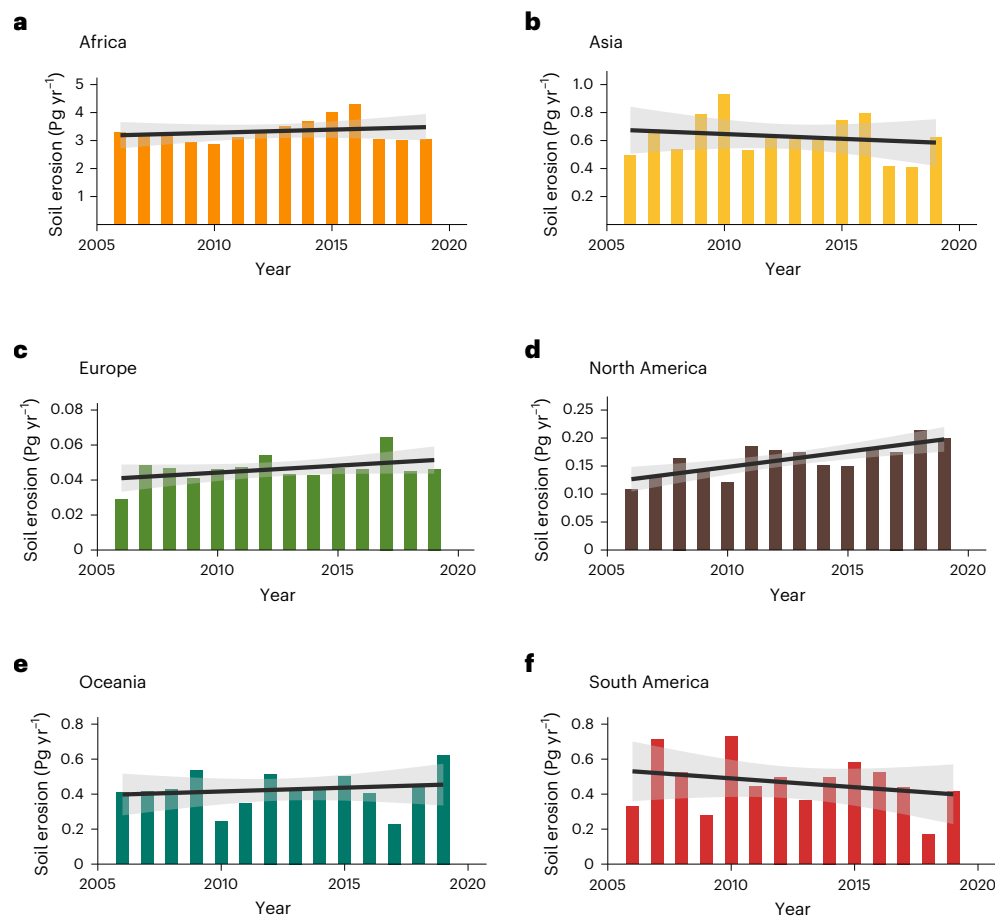


Fig. 4 | Additional post-fire soil erosion and trend per continent for consecutive fire years 2006–2019. a–f. Bars concern annual estimates of additional soil erosion between 2006 and 2019 and per continent: Africa (a), Asia (b), Europe (c), North America (d), Oceania (e) and South America (f). Additional post-fire soil erosion corresponds to the difference between post-fire soil

erosion and background soil erosion. Black line indicates soil erosion trend by linear smoothed conditional means, and shaded area represents standard error with 0.95 confidence interval (ggplot2, RStudio). Note statistical significance for increasing trend for North America (Mann–Kendall trend test, two-sided, $p < 0.008595$), and non-significant trends for remaining continents.

rainfall erosivity²³. These considerations, however, do not include the anticipated changes in fire activity⁴³, which when combined with the anticipated rainfall erosivity changes²³, were projected to increase by 68% for post-fire debris flow events, in locations where those events already took place in the past¹⁰.

The results of this study combined with the limited number of countries (USA, Spain) undertaking operational post-fire management actions globally²⁰ highlight the need for further knowledge on forest disturbances to plan and implement adequate land management in the mitigation and restoration of burned areas²¹. Field studies have shown that pre-fire fuel treatments⁴⁴, post-fire soil mitigation treatments²⁰ or post-fire restoration⁴⁵ have shown positive results in the recovery of vegetation but also for soil condition⁴⁶ after wildfire.

Despite the uncertainties (Supplementary Section 4), we provide an estimation of the post-fire soil erosion globally, contributing with two new blocks (forest and fire) to the existing high-resolution global soil erosion estimates and projections (GLoSEM)¹⁷. However, further research on how additional disturbances impact post-fire soil erosion and recovery is still required, namely, for how long wildfire affects soil properties⁴¹, what is the feedback of those fire-induced changes in forest recovery⁴⁷ and how well vegetation indices represent those dynamics. Ultimately those knowledge gaps can be implemented in soil erosion models, thus achieving more robust predictions at multiple scales and a more informed decision-making. Moreover, further investigations on offsite impacts due to the post-fire soil erosion, including the carbon sink ability of soil organic carbon redistribution by erosion

after fire⁴⁸ or the impact of the transport of sediments and ash to the downstream water bodies¹¹ are necessary.

Conclusion

This study estimates soil erosion under post-fire conditions at the global scale. The main findings of this modelling exercise with respect to the 2001–2019 burned area are as follows:

- Our study estimates global post-fire soil erosion to be 8.1 Pg yr⁻¹, considering cumulative effects of 18 years of fire disturbances.
- Post-fire soil erosion estimations correspond to 19% of the global estimation for all land and 35% of the erosion for agricultural land¹⁷.
- Africa is the continent that is impacted the most in terms of post-fire soil erosion (62%), given its substantially larger burned area (67% total).
- The standard recovery time could not be determined under this study, given the substantial proportion of areas (> 50%) presenting less vegetation cover in comparison to pre-fire conditions.
- The 2006–2019 period reveals an increasing post-fire soil erosion trend, and when using projections for 2050–2070 rainfall erosivity, post-fire soil erosion is predicted to further increase, with 11–23% and 23–28% increase, for 2050 and 2070, respectively.
- Post-fire recovery showed limited recovery after fire, especially in regions such as Africa and Europe. Countries involved should prioritize post-fire actions to prevent land degradation and adapt to future climate demands.

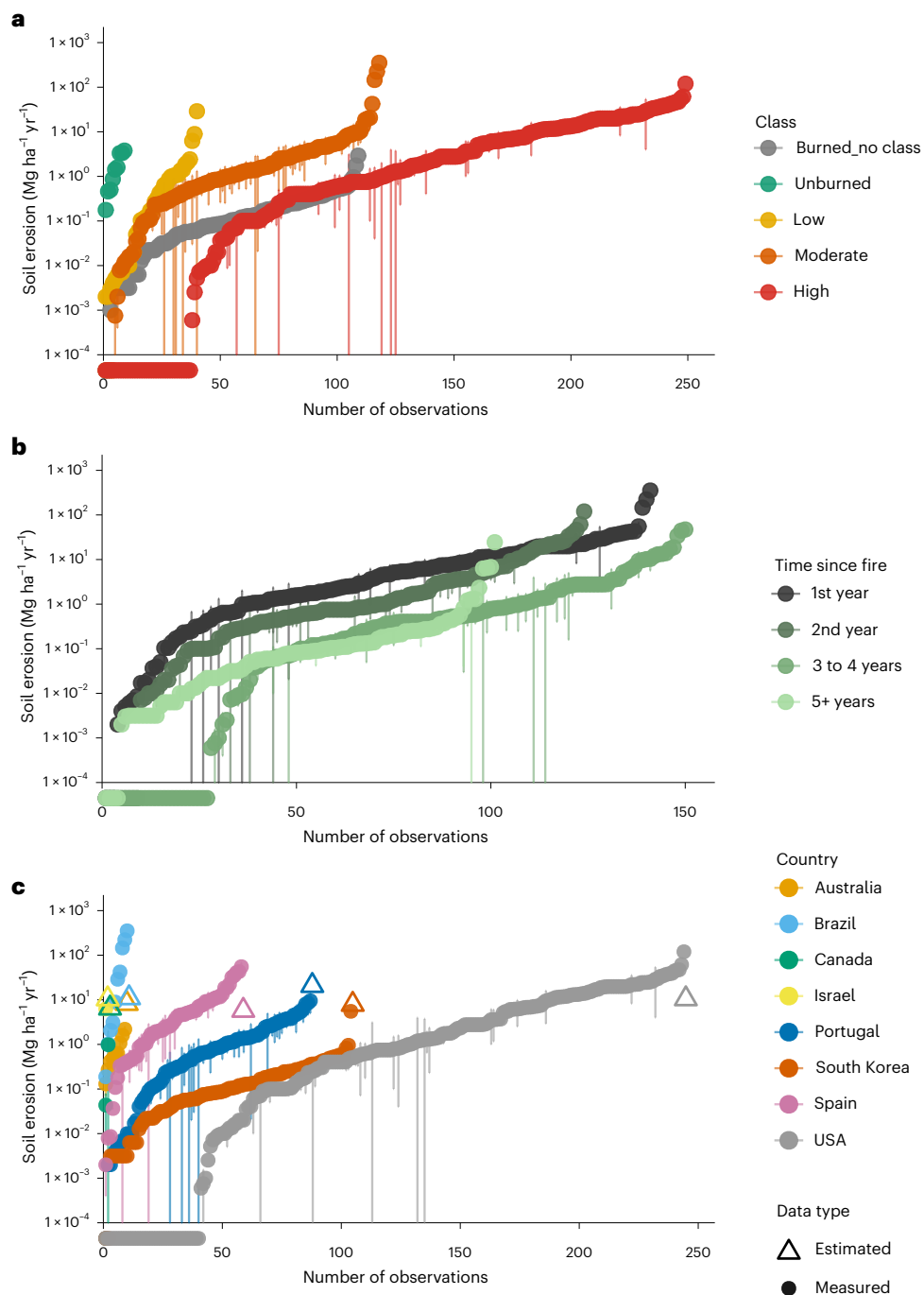


Fig. 5 | Field-measured annual post-fire soil erosion rates in $\text{Mg ha}^{-1} \text{yr}^{-1}$ under different burn severities, time since fire and from individual countries. a, Soil erosion observations ($n = 525$) per burn-severity classification (low, moderate, high) for burned areas without severity classification (Burned_no class) and for unburned conditions. **b,** Post-fire soil erosion observations ($n = 516$) per time

since fire for first, second, three to four and more than five years after fire. **c,** Post-fire soil erosion rates by country, including post-fire soil erosion-rate estimates for first post-fire year for comparison ($n = 516$). Error bars depict soil erosion standard deviation as reported in original study, if available. Data from ref. 51.

These results reinforce that limited attention has been given to the prevention and mitigation of wildfire impacts to forest soils. We suggest using these results to improve climate change assessment reports, and to inform about wildfires contributions to land-degradation reporting. Moreover, improving global forest resilience is urgent to halt land degradation and enhance climate change adaptation.

Online content

Any methods, additional references, Nature Portfolio reporting summaries, source data, extended data, supplementary information,

acknowledgements, peer review information; details of author contributions and competing interests; and statements of data and code availability are available at <https://doi.org/10.1038/s41561-025-01876-0>.

References

- San-Miguel-Ayanz, J. et al. *Global Wildfire Information System—Country Profile* (European Commission, 2023); <https://gwis.jrc.ec.europa.eu/apps/country.profile>
- Pausas, J. G. & Keeley, J. E. Wildfires as an ecosystem service. *Front. Ecol. Environ.* **17**, 289–295 (2019).

3. Ferreira, C. S. S., Seifollahi-Aghmiuni, S., Destouni, G., Ghajarnia, N. & Kalantari, Z. Soil degradation in the European Mediterranean region: processes, status and consequences. *Sci. Total Environ.* **805**, 150106 (2022).
4. Schillaci, C., Jones, A., Vieira, D., Munafò, M. & Montanarella, L. Evaluation of the United Nations Sustainable Development Goal 15.3.1 indicator of land degradation in the European Union. *Land Degrad. Dev.* **34**, 250–268 (2023).
5. Bednar-Friedl, B. et al. in *Climate Change 2022: Impacts, Adaptation and Vulnerability* (eds Pörtner, H.-O. et al.) 1817–1928 (Cambridge Univ. Press, 2022); <https://doi.org/10.1017/9781009325844.015>
6. Moody, J. A., Shakesby, R. A., Robichaud, P. R., Cannon, S. H. & Martin, D. A. Current research issues related to post-wildfire runoff and erosion processes. *Earth-Sci. Rev.* **122**, 10–37 (2013).
7. Shakesby, R. A. & Doerr, S. H. Wildfire as a hydrological and geomorphological agent. *Earth-Sci. Rev.* **74**, 269–307 (2006).
8. Vieira, D. C. S. et al. Wildfires in Europe: burned soils require attention. *Environ. Res.* **217**, 114936 (2023).
9. Vieira, D. C. S., Fernández, C., Vega, J. A. & Keizer, J. J. Does soil burn severity affect the post-fire runoff and interrill erosion response? A review based on meta-analysis of field rainfall simulation data. *J. Hydrol.* **523**, 452–464 (2015).
10. McGuire, L. A., Ebel, B. A., Rengers, F. K., Vieira, D. C. S. & Nyman, P. Fire effects on geomorphic processes. *Nat. Rev. Earth Environ.* **5**, 486–503 (2024).
11. Basso, M., Serpa, D., Mateus, M., Keizer, J. J. & Vieira, D. C. S. Advances on water quality modeling in burned areas: a review. *PLoS Water* **1**, e0000025 (2022).
12. Santi, P. M. & Rengers, F. K. in *Treatise on Geomorphology* 2nd edn (ed. Shroder, J. F.) 765–797 (Academic Press, 2022); <https://doi.org/10.1016/B978-0-12-818234-5.00017-1>
13. Lopes, A. R. et al. What is wrong with post-fire soil erosion modelling? A meta-analysis on current approaches, research gaps, and future directions. *Earth Surf. Process. Landf.* **46**, 205–219 (2021).
14. Noske, P. J., Nyman, P., Lane, P. N. J., Rengers, F. K. & Sheridan, G. J. Changes in soil erosion caused by wildfire: a conceptual biogeographic model. *Geomorphology* **459**, 109272 (2024).
15. Flores, B. M. & Holmgren, M. White-sand savannas expand at the core of the Amazon after forest wildfires. *Ecosystems* **24**, 1624–1637 (2021).
16. Nyman, P., Sheridan, G. J. & Lane, P. N. J. Hydro-geomorphic response models for burned areas and their applications in land management. *Prog. Phys. Geogr. Earth Environ.* **37**, 787–812 (2013).
17. Borrelli, P. et al. Land use and climate change impacts on global soil erosion by water (2015–2070). *Proc. Natl Acad. Sci. USA* **117**, 21994–22001 (2020).
18. Borrelli, P. et al. An assessment of the global impact of 21st century land use change on soil erosion. *Nat. Commun.* **8**, 2013 (2017).
19. Alonso-González, E. & Fernández-García, V. MOSEV: a global burn severity database from MODIS (2000–2020). *Earth Syst. Sci. Data* **13**, 1925–1938 (2021).
20. Girona-García, A. et al. Effectiveness of post-fire soil erosion mitigation treatments: a systematic review and meta-analysis. *Earth-Sci. Rev.* **217**, 103611 (2021).
21. Antwi, E. K. et al. A global review of cumulative effects assessments of disturbances on forest ecosystems. *J. Environ. Manage.* **317**, 115277 (2022).
22. Patacca, M. et al. Significant increase in natural disturbance impacts on European forests since 1950. *Glob. Change Biol.* **29**, 1359–1376 (2023).
23. Panagos, P. et al. Global rainfall erosivity projections for 2050 and 2070. *J. Hydrol.* **610**, 127865 (2022).
24. Lopez, A. M. et al. Molecular insights and impacts of wildfire-induced soil chemical changes. *Nat. Rev. Earth Environ.* **5**, 431–446 (2024).
25. Cerdá, A. & Doerr, S. H. Influence of vegetation recovery on soil hydrology and erodibility following fire: an 11-year investigation. *Int. J. Wildland Fire* **14**, 423–437 (2005).
26. Robichaud, P. R., Lewis, S. A., Wagenbrenner, J. W., Brown, R. E. & Pierson, F. B. Quantifying long-term post-fire sediment delivery and erosion mitigation effectiveness. *Earth Surf. Process. Landf.* **45**, 771–782 (2020).
27. Wittenberg, L. & Inbar, M. The role of fire disturbance on runoff and erosion processes—a long-term approach, Mt. Carmel case study. *Isr. Geogr. Res.* **47**, 46–56 (2009).
28. Vieira, D. C. S., Malvar, M. C., Fernández, C., Serpa, D. & Keizer, J. J. Annual runoff and erosion in a recently burn Mediterranean forest—the effects of plowing and time-since-fire. *Geomorphology* **270**, 172–183 (2016).
29. Verheijen, F. G. A., Jones, R. J. A., Rickson, R. J. & Smith, C. J. Tolerable versus actual soil erosion rates in Europe. *Earth-Sci. Rev.* **94**, 23–38 (2009).
30. Girona-García, A. et al. How much does it cost to mitigate soil erosion after wildfires?. *J. Environ. Manage.* **334**, 117478 (2023).
31. Parente, J., Girona-García, A., Lopes, A. R., Keizer, J. J. & Vieira, D. C. S. Prediction, validation, and uncertainties of a nation-wide post-fire soil erosion risk assessment in Portugal. *Sci. Rep.* **12**, 2945 (2022).
32. Basso, M., Vieira, D. C. S., Ramos, T. B. & Mateus, M. Assessing the adequacy of SWAT model to simulate postfire effects on the watershed hydrological regime and water quality. *Land Degrad. Dev.* **31**, 619–631 (2020).
33. Basso, M., Baartman, J., Martins, M., Keizer, J. & Vieira, D. Predicting post-fire hydrological and erosive catchment response during rainfall events. A comparison of OpenLISEM and MOHID Land models. *J. Hydrol.* **636**, 131258 (2024).
34. Fernández-Guisuraga, J. M., Martins, S. & Fernandes, P. M. Characterization of biophysical contexts leading to severe wildfires in Portugal and their environmental controls. *Sci. Total Environ.* **875**, 162575 (2023).
35. Archibald, S., Lehmann, C. E. R., Gómez-Dans, J. L. & Bradstock, R. A. Defining pyromes and global syndromes of fire regimes. *Proc. Natl Acad. Sci. USA* **110**, 6442–6447 (2013).
36. Forzieri, G., Dakos, V., McDowell, N. G., Ramdane, A. & Cescatti, A. Emerging signals of declining forest resilience under climate change. *Nature* **608**, 534–539 (2022).
37. Xu, H. et al. Global patterns and drivers of post-fire vegetation productivity recovery. *Nat. Geosci.* **17**, 874–881 (2024).
38. Prosser, I. P. & Williams, L. The effect of wildfire on runoff and erosion in native Eucalyptus forest. *Hydrol. Processes* **12**, 251–265 (1998).
39. Wittenberg, L., Malkinson, D. & Barzilai, R. The differential response of surface runoff and sediment loss to wildfire events. *Catena* **121**, 241–247 (2014).
40. Wagenbrenner, J. W., Ebel, B. A., Bladon, K. D. & Kinoshita, A. M. Post-wildfire hydrologic recovery in Mediterranean climates: a systematic review and case study to identify current knowledge and opportunities. *J. Hydrol.* **602**, 126772 (2021).
41. Garcia-Braga, E., Peñalver-Alcalá, A., Farguella, J., Francos, M. & Úbeda, X. How long is long? A bibliographic review of what is meant by the long-term effects of fire on soil properties. *Span. J. Soil Sci.* **14**, 12499 (2024).
42. He, K., Shen, X. & Anagnostou, E. Global burn severity in forest ecoregions: trends, climate drivers, and predictive insights. *npj Nat. Hazards* **2**, 61 (2025).

43. Senande-Rivera, M., Insua-Costa, D. & Miguez-Macho, G. Spatial and temporal expansion of global wildland fire activity in response to climate change. *Nat. Commun.* **13**, 1208 (2022).
44. Fernández-Guisuraga, J. M. & Fernandes, P. M. Enhanced post-wildfire vegetation recovery in prescribed-burnt Mediterranean shrubland: a regional assessment. *For. Ecol. Manage.* **561**, 121921 (2024).
45. Lopes, L. F., Dias, F. S., Fernandes, P. M. & Acácio, V. A remote sensing assessment of oak forest recovery after postfire restoration. *Eur. J. For. Res.* **143**, 1001–1014 (2024).
46. De la Rosa, J. M. et al. Mulching-induced preservation of soil organic matter quality in a burnt eucalypt plantation in central Portugal. *J. Environ. Manage.* **231**, 1135–1144 (2019).
47. Inbar, A., Nyman, P., Lane, P. N. J. & Sheridan, G. J. The role of fire in the coevolution of soils and temperate forests. *Water Resour. Res.* **56**, e2019WR026005 (2020).
48. Girona-García, A., Vieira, D., Doerr, S., Panagos, P. & Santín, C. Into the unknown: the role of post-fire soil erosion in the carbon cycle. *Glob. Change Biol.* **30**, e17354 (2024).
49. Kottke, M., Grieser, J., Beck, C., Rudolf, B. & Rubel, F. World map of the Köppen-Geiger climate classification updated. *Meteorol. Z.* **15**, 259–263 (2006).
50. Vieira, D. et al. Global Dataset of cumulative post fire soil erosion estimates (2001–2019) [Data set]. *Zenodo* <https://doi.org/10.5281/zenodo.17404150> (2025).
51. Vieira, D. & Girona-García, A. Post-fire soil erosion measurements from field plots [Data set]. *Zenodo* <https://doi.org/10.5281/zenodo.17405290> (2025).

Publisher's note Springer Nature remains neutral with regard to jurisdictional claims in published maps and institutional affiliations.

Open Access This article is licensed under a Creative Commons Attribution-NonCommercial-NoDerivatives 4.0 International License, which permits any non-commercial use, sharing, distribution and reproduction in any medium or format, as long as you give appropriate credit to the original author(s) and the source, provide a link to the Creative Commons licence, and indicate if you modified the licensed material. You do not have permission under this licence to share adapted material derived from this article or parts of it. The images or other third party material in this article are included in the article's Creative Commons licence, unless indicated otherwise in a credit line to the material. If material is not included in the article's Creative Commons licence and your intended use is not permitted by statutory regulation or exceeds the permitted use, you will need to obtain permission directly from the copyright holder. To view a copy of this licence, visit <http://creativecommons.org/licenses/by-nc-nd/4.0/>.

© European Union, represented by The European Union and Pasquale Borrelli, Simone Scarpa, Leonidas Liakos 2026

Methods

Methodological approach

To accomplish a global post-fire soil erosion assessment, this study used as main data sources land and climate data products from previous soil erosion assessments at European^{8,52} and global scales^{18,53} and remote sensing data for the determination of wildfires' impact on ecosystems and the correspondent vegetation dynamics from pre-fire conditions to post-fire recovery (Fig. 5).

The data are used to feed the Revised Universal Soil Loss Equation (RUSLE)^{54,55} for forest, shrubland and grasslands⁵⁶, following up the latest EU post-fire soil erosion assessment⁸ methodology. However, this study goes a step further by upscaling the previous methodology to the global spatial scale and by increasing the assessment temporal scale from 5 to 18 years. In addition, it also looks into the cumulative impacts of wildfires on soil erosion for several fire years (Fig. 1a–c), instead of following the recovery of a single year of fires, which was highlighted as a major underestimations aspect (Fig. 1d,e).

With the increase in the spatial and temporal scale, several adaptations were required as a result from data availability restrictions over two main data inputs, the biophysical parameter fraction of vegetation cover (FCOVER) and the normalized burn ratio (NBR). The methodological approach presents a balance between keeping a reasonable input resolution and the increase in data processing for a global study (Extended Data Figs. 5 and 6).

The FCOVER determination was required for each individual fire throughout the 18 years because the FCOVER products from Copernicus were not available before 2014. As a result, this indicator had to be estimated for all burned areas in the entire globe⁵⁷ (30-m resolution), which also gave us the opportunity to compensate the resolution loss from now using MOSEV (500 m) database¹⁹. The decision to use MOSEV database was driven by being the only open-access product compiling burned-area delineation at a global scale and by the fact that such a dataset already contained NBR classification. Moreover, a recent study has also revealed the use of FCOVER as having a good performance assessing burn severity⁵⁸. Because such changes could lead to new uncertainties, and because it was possible to replicate the original⁸ assessment under this new methodology, the soil erosion results under both methodologies were compared to assess quality (Supplementary Section 3).

RUSLE model and pre-fire conditions

This study used the RUSLE^{54,55} to model the average soil erosion potential in the absence of wildfire by including ground-cover changes described by ref. 59. The RUSLE model uses the following factors to estimate soil loss:

$$A = R \times K \times LS \times C \times P \quad (1)$$

where A is the soil loss ($\text{Mg ha}^{-1} \text{yr}^{-1}$), R is the rainfall and runoff factor ($\text{MJ mm h}^{-1} \text{ha}^{-1} \text{yr}^{-1}$), K is the soil erodibility factor ($\text{Mg h MJ}^{-1} \text{mm}^{-1}$), LS is the slope length and the slope steepness factor (dimensionless) and $C \times P$ is the cover management practice factor (dimensionless).

The K and R factors were expressed spatially using the latest maps created by the Joint Research Centre of the European Commission⁵³. The C —cover and management—factor was originally developed for agricultural croplands. It has to be adjusted to forest, shrub and grasslands ground-cover characteristics to be able to spatially differentiate the various cover species, canopy cover densities and ground-floor vegetation⁵². Considering the size of the study area, the C factor used to predict the soil loss potential⁸ was quantified by manipulating the biophysical parameter Fraction of Vegetation Cover (FCOVER⁶⁰). This provided an estimation of the fraction of the vegetation that is visible vertically, allowing to differentiate a C factor for undisturbed conditions (C_U) between bare or protected soil for forest, shrub and

grasslands (Extended Data Fig. 5). Management practices (P) were not considered under this assessment.

Adaptation for post-fire conditions

With regard to the wildfire disturbance, the state of the art identified that post-fire soil erosion rates and vegetation recovery are closely related to burnt severity and bare soil cover^{9,20}. Notwithstanding, as shown by previous research^{61,62}, forests, shrubland and grasslands are distinctively impacted by wildfires, whereas contrary to the undisturbed condition, burned forests present much higher post-fire soil erosion rates in comparison to shrubland and grasslands due to higher fire residence times and burn severities. Therefore, the C factor for burned conditions (Fig. 1) was approximated as follows:

$$C_{\text{max}_B, \text{Forest}} = C_{\text{max}_U, \text{Forest}} \times B_{\text{severity}} \times 10 \text{ for FCOVER} = 0.2, \text{ max} = 0.5 \quad (2)$$

$$C_{\text{max}_B, \text{Shrub}} = C_{\text{max}_U, \text{Shrub}} \times B_{\text{severity}} \text{ for FCOVER} = 0.2, \text{ max} = 0.3 \quad (3)$$

$$C_{\text{max}_B, \text{Grass}} = C_{\text{max}_U, \text{Grass}} \times B_{\text{severity}} \text{ for FCOVER} = 0.2, \text{ max} = 0.3 \quad (4)$$

where, for equations (2), (3) and (4), the maximum C factor for burned conditions (C_{max_B}) was estimated by multiplying the maximum C factor for undisturbed conditions (C_{max_U}) and the burn-severity anomaly factor (B_{severity}) as previously derived through effect size determination for erosive response between burned and unburned conditions⁹. Such a maximum value was determined for ground-cover (FCOVER) values of 0.2, similarly to previous approach⁶³. Regarding the individual cover types, for forest (equation (2)) the C factor was increased one order of magnitude for all the severities and limited to a maximum of 0.5, while shrubland (equation (3)) and grasslands (equation (4)) were represented by low and moderate severities and limited to a maximum of 0.3. In this way, it was possible to accommodate the impacts determined for distinctive severities⁹, and also the conceptual model⁶² for hydrological response and observations on soil properties⁶¹ for distinct cover types (Extended Data Fig. 6).

The recovery of the burned areas was addressed by using vegetation cover indicators as proxies, resulting our definition for recovery⁸, which considers that an area is recovered once the ground cover reaches the pre-fire conditions. In this way, it was possible to determine the erosion reduction with the increase of the protective cover but also to consider the initial characteristics of the local vegetation before the wildfires.

For the first point, a minimum C factor was estimated:

$$C_{\text{min}_B} = C_{\text{min}_U} \text{ for FCOVER} = 1.0 \quad (5)$$

Being the minimum C factor for burned conditions, C_{min_B} approximated to the C_{min_U} (ref. 52) for each land cover (forest = 0.0001, shrubland = 0.003 and grassland = 0.01) whenever the ground cover (FCOVER) reached its maximum value of 1.

This formulation allowed for the inclusion of the impact of the burn severity in the soil erosion estimations for when protective cover presented the minimum value according to the burn-severity impact and the approximation of the recovery of the burned areas under an exponential curve in the function of FCOVER over the monitoring period (Extended Data Figs. 5 and 6 and Supplementary Section 5). The choice of an exponential base for such estimations goes in line with the conceptual model after observing a nonlinear relationship between sediment yields and bare soil cover⁶² and a sharp increase of the sediment yields on the 60–70% bare soil cover⁹.

Therefore a recovery rate (RCOVER) was calculated, and several classes (Extended Data Table 1) were defined as follows:

$$\text{RCOVER}_t = \frac{\text{FCOVER}_t}{\text{FCOVER}_{\text{pre-fire}}} \quad (6)$$

The consideration of a RCOVER class allowed us to adopt a succession of *C* factor equations according to the status of the vegetation-recovery progress (Supplementary Section 5). For the first two classes 'No Recovery' and 'Ongoing Recovery', the *C* factor would be calculated as described for equations (2)–(5), according to the initial burn-severity classification and land-cover attributes. In the case of 'Near Recovery' class, this would lead to the adoption of the equation with one burn-severity level lower than the original one; likewise the 'Recovered' class would lead to adoption of the equation corresponding to unburned conditions. This formulation allowed us to use FCOVER as a constant input for *C* estimations, while reducing the impact of severity proportionally to the pre-fire conditions.

Spatial data processing

The burned-area delineation, wildfire date and burn severity (NBR) were retrieved from the MOSEV database¹⁹ with a resolution of 500 m and global coverage, for the 2000–2020 period for all fires with an area of at least 25 ha. Given the incompleteness of the dataset for the years of 2000 and 2020, these were removed from our analysis, whereas burn severity was then converted to low, moderate and high burn-severity classes⁵⁴.

To target the land-cover types affected by wildfires, the reference dataset for land-cover fractions, the dynamic land-cover map at 100-m resolution (CGLS-LC100⁵⁶) was used, which allowed estimation of the individual contributions of soil erosion for forest, shrub and grassland with a reference year of 2015. Despite a more recent version of this dataset existing (2019), the choice to keep 2015 was made to keep the comparability with the previous assessment⁸, but also because of the inexistence of comparable datasets before this date, which would allow accommodation of land-cover changes throughout the entire temporal scale of this study. Nonetheless, to ensure consistency, both land-cover datasets for 2015 and 2019 were compared for the total area affected by fire (17 million km²), resulting in land-cover changes (difference in cover share (%) in each pixel) under the ± 10% threshold. Moreover, cropland was also excluded from this analysis due to the lack of consolidated knowledge on the cumulative effect from intensive soil management operations and wildfire⁸, whereas at the same time, soil erosion in these areas have already been assessed extensively¹⁷.

The ground-cover changes were assessed with FCOVER⁶⁰, which provides a measure of the fraction of ground covered by green vegetation. The change in vegetation cover at 30-m resolution was determined by Normalized Differential Vegetation Index (NDVI⁵⁷), using as a reference the date the first Landsat imagery was available following each fire record. The repeated measurement of NDVI was performed annually (2001–2019) to follow up the recovery of each burned area. Whenever a repeated wildfire occurred in the same location, the procedure would start again considering the latest fire as a reference and assuming the recovery was sufficient to allow the most recent fire to occur.

Data availability

The dataset for global pre- and post-fire soil erosion (2001–2019) is available via Zenodo at <https://doi.org/10.5281/zenodo.17404150> (ref. 50). The dataset for post-fire soil erosion measurements from field plots is available via Zenodo at <https://doi.org/10.5281/zenodo.17405290> (ref. 51).

References

52. Panagos, P. et al. The new assessment of soil loss by water erosion in Europe. *Environ. Sci. Policy* **54**, 438–447 (2015).

53. Borrelli, P., Ballabio, C., Yang, J. E., Robinson, D. A. & Panagos, P. GloSEM: high-resolution global estimates of present and future soil displacement in croplands by water erosion. *Sci. Data* **9**, 406 (2022).
54. Renard, K., Foster, G. R., Weesies, G., McCool, D. & Yoder, D. *Predicting Soil Erosion by Water: A Guide to Conservation Planning with the Revised Universal Soil Loss Equation* (RUSLE) (USDA, 1997).
55. Renard, K. G., Yoder, D. C., Lightle, D. T. & Dabney, S. M. in *Handbook of Erosion Modelling* 135–167 (John Wiley & Sons, Ltd, 2010); <https://doi.org/10.1002/9781444328455.ch8>
56. Buchhorn, M. et al. Copernicus Global Land Service: land Cover 100 m: version 3 globe 2015–2019: product user manual. Zenodo <https://doi.org/10.5281/zenodo.3938963> (2020).
57. Song, D.-X., Wang, Z., He, T., Wang, H. & Liang, S. Estimation and validation of 30 m fractional vegetation cover over China through integrated use of Landsat 8 and Gaofen 2 data. *Sci. Remote Sens.* **6**, 100058 (2022).
58. Fernández-Guisuraga, J. M., Calvo, L., Quintano, C., Fernández-Manso, A. & Fernandes, P. M. Fractional vegetation cover ratio estimated from radiative transfer modeling outperforms spectral indices to assess fire severity in several Mediterranean plant communities. *Remote Sens. Environ.* **290**, 113542 (2023).
59. Hansen, M. C. et al. High-resolution global maps of 21st-century forest cover change. *Science* **342**, 850–853 (2013).
60. Fuster, B. et al. Quality Assessment of PROBA-V LAI, fAPAR and fCOVER Collection 300 m products of Copernicus Global Land Service. *Remote Sens.* **12**, 1017 (2020).
61. Cheng, G. et al. Fire differentially affects soil properties of forests and grasslands: a global meta-analysis. *CATENA* **255**, 109031 (2025).
62. Johansen, M. P., Hakonson, T. E. & Breshears, D. D. Post-fire runoff and erosion from rainfall simulation: contrasting forests with shrublands and grasslands. *Hydrol. Processes* **15**, 2953–2965 (2001).
63. Wischmeier, W. H. & Smith, D. D. *Predicting Rainfall Erosion Losses. A Guide to Conservation Planning. The USDA Agricultural Handbook No. 537* (USDA, 1978).
64. Key, C. & Benson, N. *Landscape Assessment: Ground Measure of Severity, the Composite Burn Index, and Remote Sensing of Severity, the Normalized Burn Ratio* (USGS, 2006).
65. Olson, D. M. et al. Terrestrial ecoregions of the world: a new map of life on Earth. *BioScience* **51**, 933–938 (2001).

Acknowledgements

We thank P. Fernandes and F. Matthews for helpful discussions. The authors received no specific funding for this work. P.B. acknowledges support for this work by the Swiss State Secretariat for Education, Research and Innovation (SERI), grant number 101157867 – MONALISA.

Author contributions

D.C.S.V.: conceptualization, methodology, data curation, formal analysis, writing—original draft and writing—review and editing. P.B.: conceptualization, methodology, writing—original draft and writing—review and editing. S.S.: data curation and formal analysis. L.L.: data curation and formal analysis. C.B.: conceptualization, methodology and writing—review and editing. P.P.: conceptualization, writing—original draft and writing—review and editing.

Competing interests

The authors declare no competing interests.

Additional information

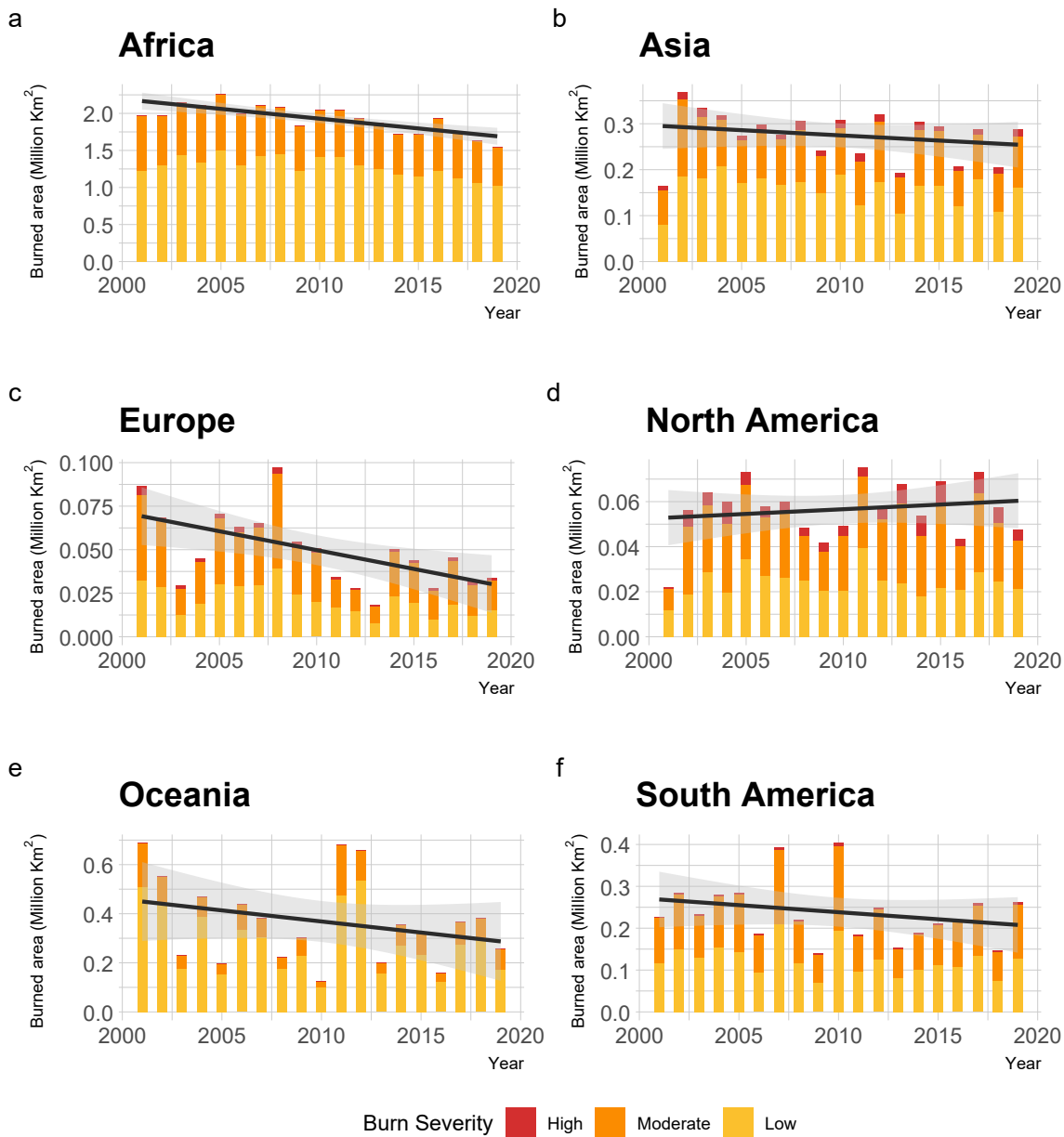
Extended data is available for this paper at <https://doi.org/10.1038/s41561-025-01876-0>.

Supplementary information The online version contains supplementary material available at <https://doi.org/10.1038/s41561-025-01876-0>.

Correspondence and requests for materials should be addressed to D. C. S. Vieira.

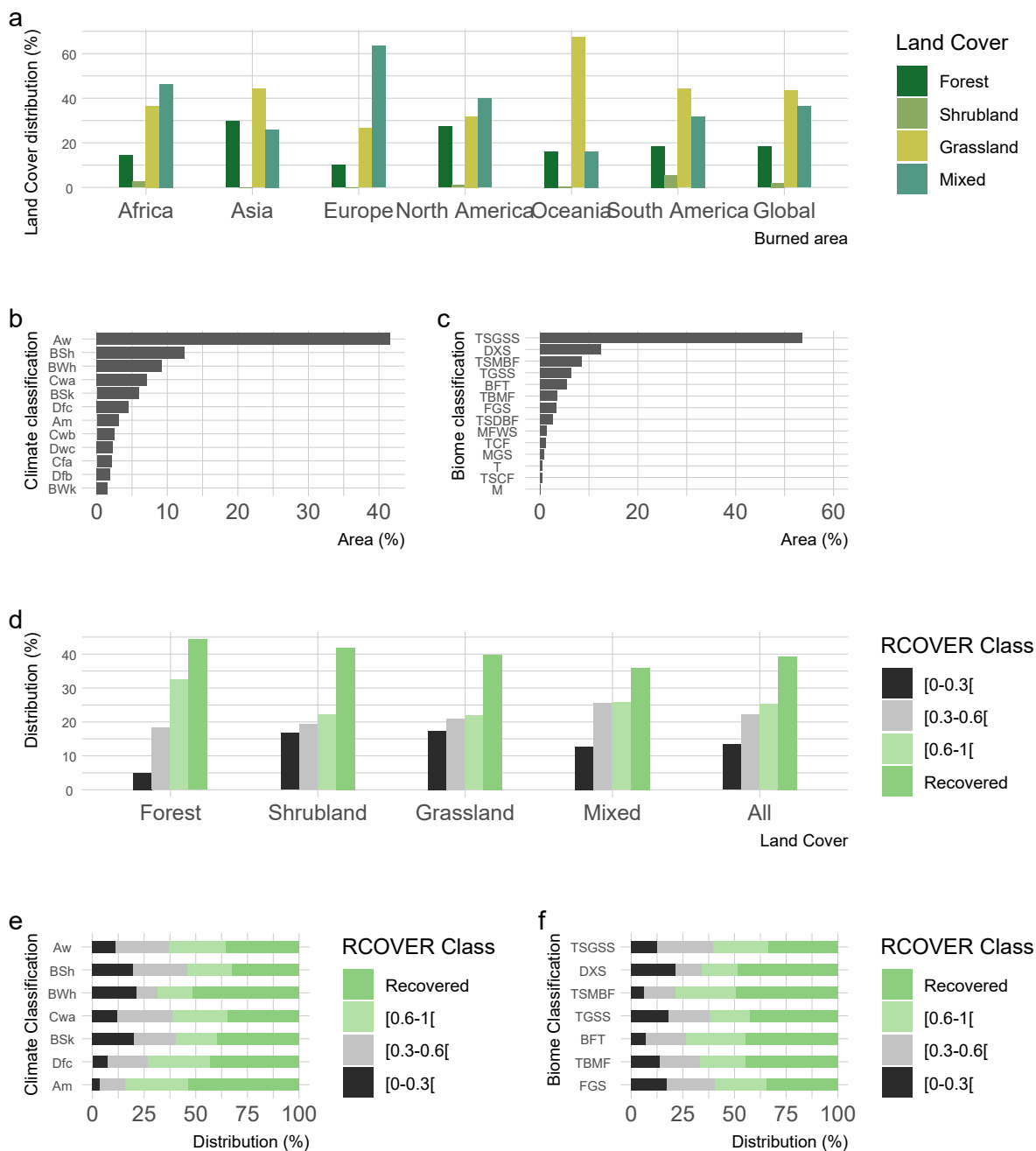
Peer review information *Nature Geoscience* thanks Longxi Cao, Lea Wittenberg and the other, anonymous, reviewer(s) for their contribution to the peer review of this work. Primary Handling Editors: Tamara Goldin and Carolina Ortiz-Guerrero, in collaboration with the *Nature Geoscience* team.

Reprints and permissions information is available at www.nature.com/reprints.



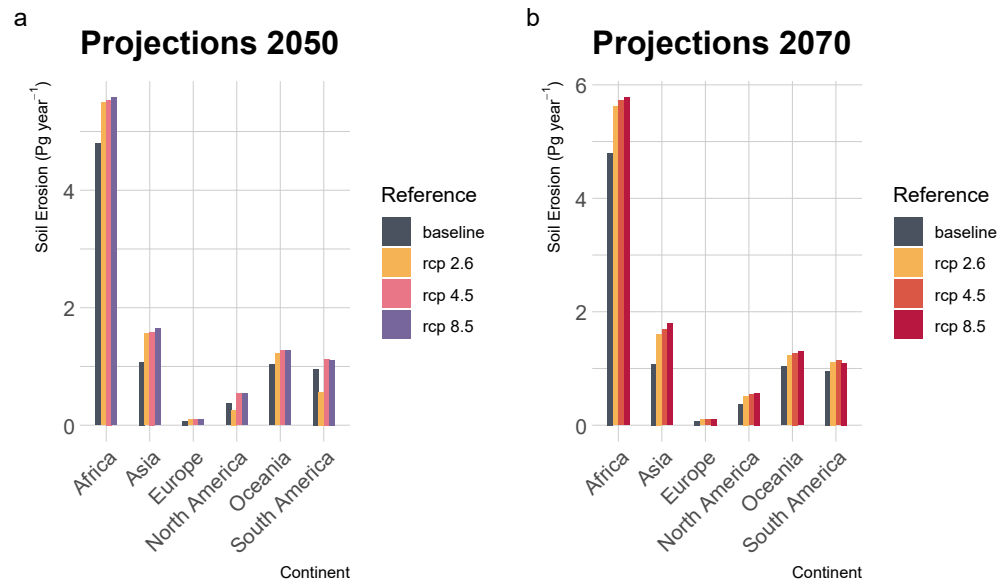
Extended Data Fig. 1 | Annual trends in burned area by continent (Million km²). **a**, Total annual burned area, trend, and severity for Africa. **b**, Total annual burned area, trend, and severity for Asia. **c**, Total annual burned area, trend, and severity for Europe. **d**, Total annual burned area, trend, and severity for North-America. **e**, Total annual burned area, trend, and severity for Oceania. **f**, Total annual burned area, trend, and severity for South America. Total annual burned area

and severity from MOSEV data¹⁹ for forest, shrubland and grassland cover. Levels of burn severity based on Normalized Burn Ratio (NBR) thresholds⁶⁴. Black line indicates long-term annual burned area trend by linear smoothed conditional means shaded area represents standard error with 0.95 confidence interval (ggplot2, RStudio).

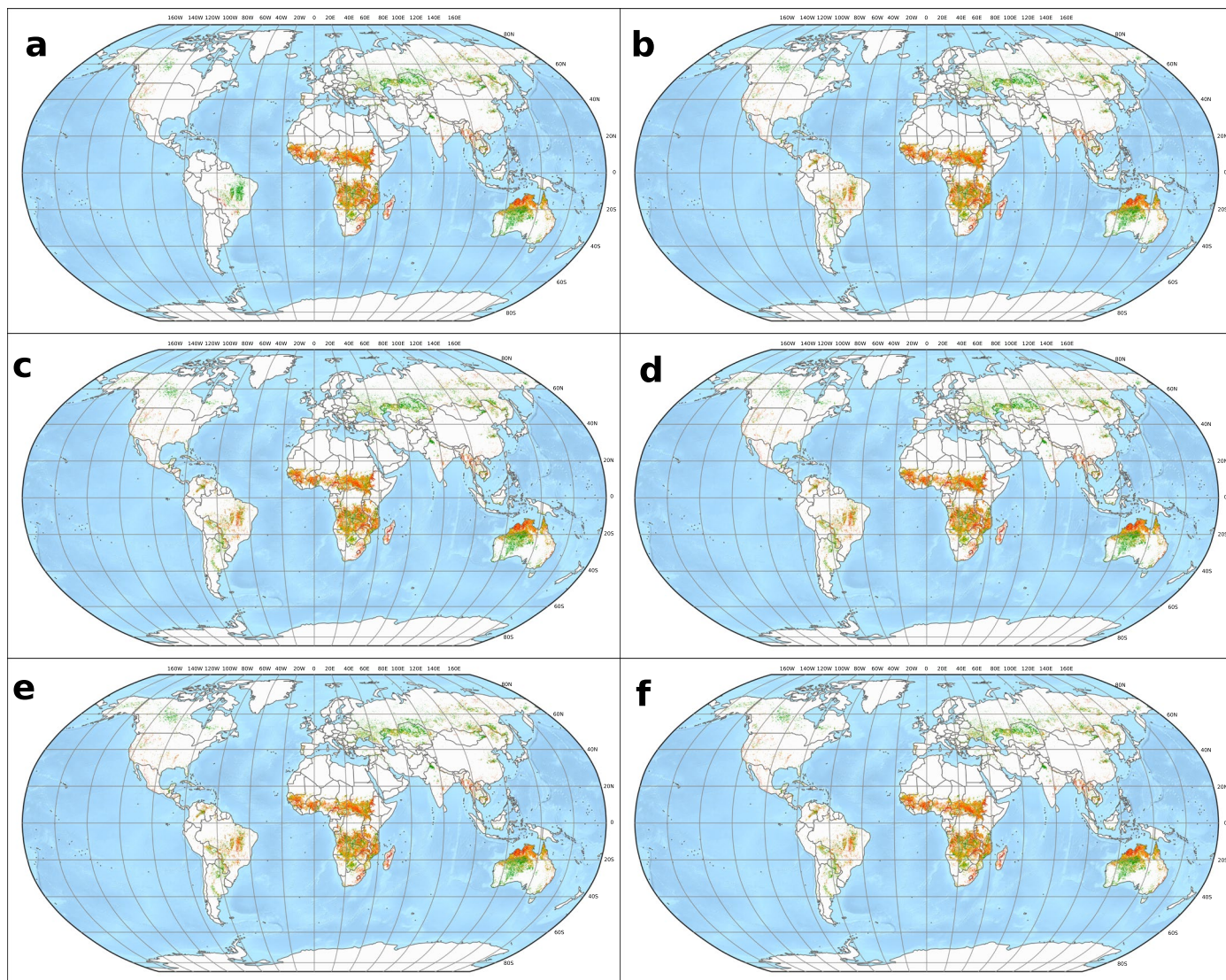


Extended Data Fig. 2 | Land Cover (%), Climate (%), Biome (%), and RCOVER (%) characterization for the 2019 cumulative burned area. a, Land Cover distribution (%) (Forest, Shrubland, Grassland). **b**, Top 12 fire affected Climates⁴⁹. **c**, Fire affected Biomes⁶⁵. **d**, RCOVER distribution (%) per Land Cover. **e**, RCOVER distribution (%) per top 7 affected Climates⁴⁹. **f**, RCOVER distribution (%) per

top 7 affected Biomes⁶⁵. Note Land Cover for forest, shrubland, and grassland correspond to areas dominated by these land cover (> 50%), otherwise classified as mixed. RCOVER classes: [0-0.3[- No Recovery, [0.3-0.6[- Ongoing Recovery, [0.6-1.0[- Near recovery, and RCOVER > 1 - Recovered.



Extended Data Fig. 3 | Continental post-fire soil erosion estimation under the 2.6, 4.5, and 8.5 RCP scenarios. a, Post-fire soil erosion for 2050. **b,** Post-fire soil erosion for 2070. Note the post-fire soil erosion estimation for 2019 as reference.



Post-fire soil erosion projections (Mg ha^{-1})



<1

1-3

3-5

5-10

10-20

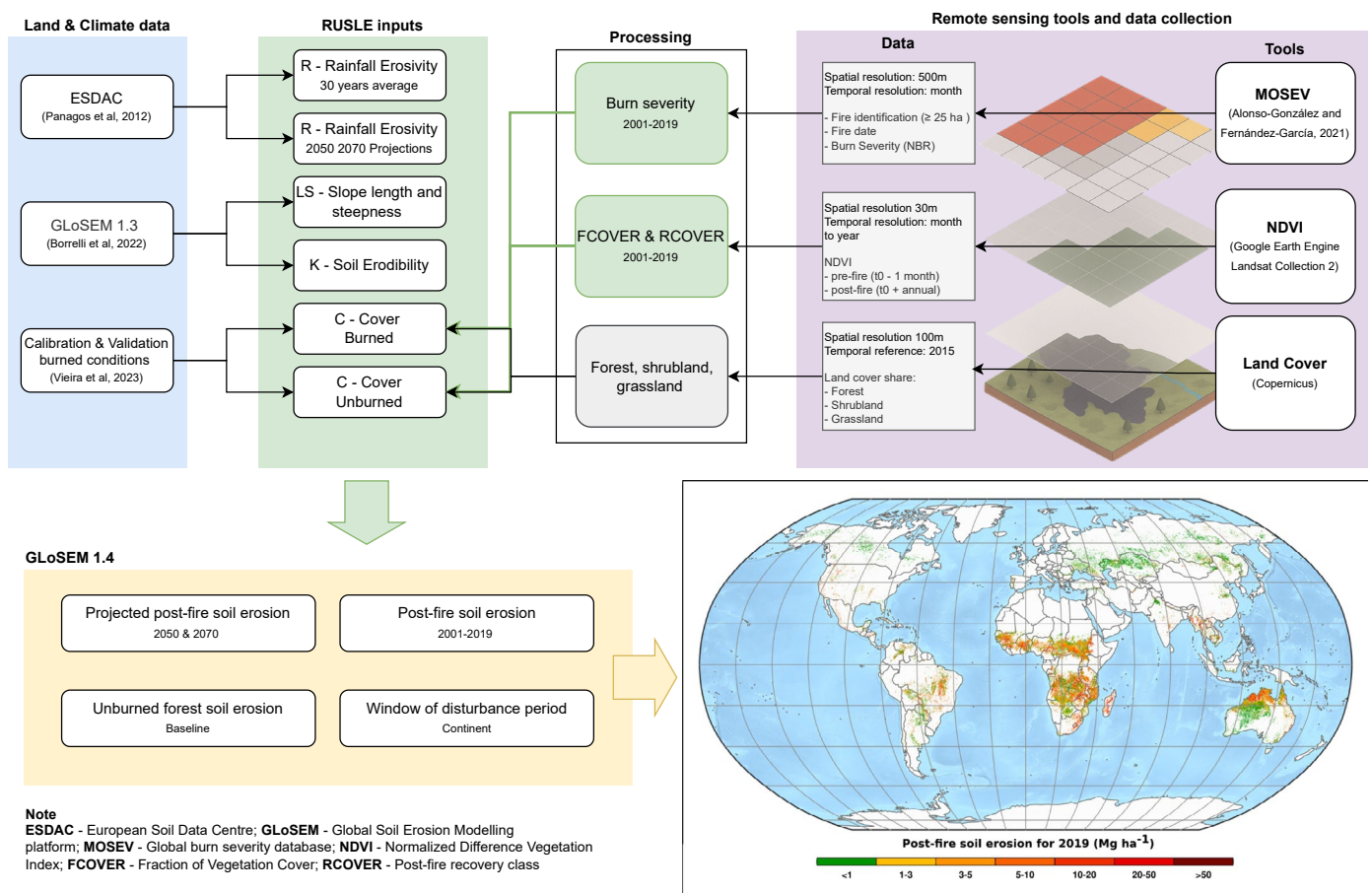
20-50

>50

Extended Data Fig. 4 | Global post-fire soil erosion estimation in burned areas for 2050 and 2070 under the 2.6, 4.5, and 8.5 RCP scenarios. **a**, Post-fire soil erosion estimation for 2050 under RCP 2.6. **b**, Post-fire soil erosion estimation for 2070 under RCP 2.6. **c**, Post-fire soil erosion estimation for 2050 under RCP 4.5. **d**, Post-fire soil erosion estimation for 2070 under RCP 4.5. **e**, Post-fire soil erosion estimation for 2050 under RCP 8.5. **f**, Post-fire soil erosion estimation for

2070 under RCP 8.5. Using post-fire soil erosion estimates for 2019 as baseline, future projections in post-fire soil erosion include anticipated global changes in Rainfall Erosivity²³. Soil erosion rates are categorized into seven classes based on the European Soil Bureau classification and the Global Soil Erosion Modelling Framework (GloSEM)¹⁷. Basemaps from Natural Earth (naturalearthdata.com) (projected coordinate system: sphere Robinson).

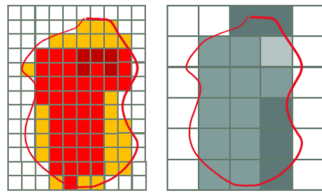
Global post-fire soil erosion modeling approach GLoSEM1.4



Extended Data Fig. 5 | Overall methodological modelling approach. Scheme of data sources, model inputs, tools and processing for the global estimation of post-fire soil erosion. Post-fire soil erosion map from Fig. 2b. Illustration created with draw.io (v28.2.8).

Methods applied in Vieira et al 2023

Spatial Scale: EU
 Temporal scale: Annual (5 years)
 Number Events: 2,679 individual fires

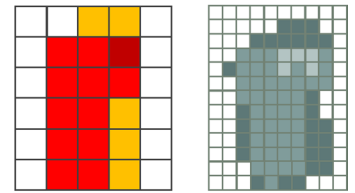


NBR 25m resolution (individual fire)
 FCOVER 300m resolution

Pros: Clear delineation of fire perimeter as provided by EFFIS. FCOVER products available since 2014.
Cons: Labor intensive determining NBR for individual fires.

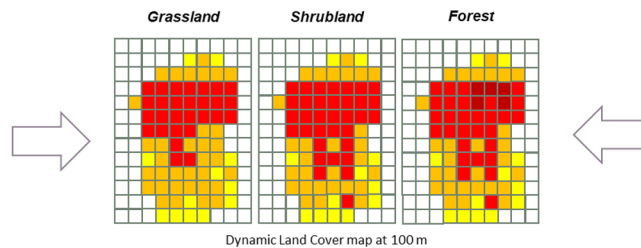
Methods applied in current study

Spatial Scale: Global
 Temporal scale: Annual (18 years)
 Number Events: 80,506,100 fires (approx.)

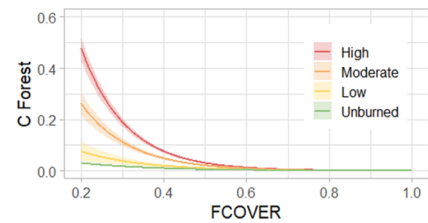
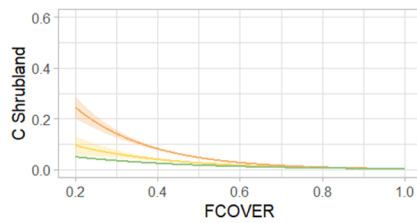
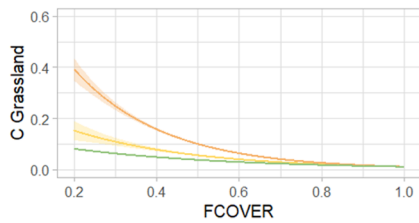


NBR 500m resolution (MOSEV)
 FCOVER 30m resolution (individual burn pixel)

Pros: Long-term data availability (18 years). Applicable at global scale.
Cons: Underestimation small fires (MOSEV). Labour intensive FCOVER processing due to lack of historical products.



Apply dedicated calibrated equations per land cover type



Extended Data Fig. 6 | Methodological adaptation to new spatial and temporal scales focusing in FCOVER and NBR dataset. Major changes are the alteration of NBR from 25 m to 500 m resolution, and the FCOVER from 300 m to 30 m. C factors derived¹⁰ for unburned and burned conditions for forest, shrubland, grassland, and cropland, according to low, moderate and high burn severity.

Extended Data Table 1 | RCOVER classification¹⁰

RCOVER classification	RCOVER
No Recovery	[0.0 - 0.3 [
Ongoing Recovery	[0.3 - 0.6[
Near Recovery	[0.6 - 1.0[
Recovered	≥ 1.0